Polymorphism in the *MAGI2* Gene Modifies the Effect of Amyloid β on Neurodegeneration

Hang-Rai Kim, MD,†‡ Taeyeop Lee, MD,*§ Jung K. Choi, PhD,‖ Yong Jeong, MD,*†‖ and for the Alzheimer's Disease Neuroimaging Initiative*

Introduction: A weak association between amyloid β (Aβ) deposition and neurodegeneration biomarkers, such as brain atrophy, has been repeatedly reported in a subset of patients with Alzheimer disease, suggesting individual differences in response to Aβ deposition.

Methods: Here, we performed a genome-wide interaction study to identify single-nucleotide polymorphism (SNP) that modify the effect of Aβ (measured by ^{18}F-florbetapir positron emission tomography) on brain atrophy (measured by cortical thickness using magnetic resonance imaging). We used magnetic resonance imaging, positron emission tomography, cerebrospinal fluid, and genetic data from the Alzheimer's Disease Neuroimaging Initiative (ADNI) database [discovery cohort, ADNI-GO/2 (n = 723) and replication cohort, ADNI-1 (n = 129)].

Results: We identified a genome-wide suggestive interaction of rs3807779 SNP ($\beta = -0.14$, SE = 0.029, $P = 9.08\times10^{-7}$) in the discovery cohort. The greater dosage of rs3807779 SNP increased the detrimental effect of Aβ deposition on cortical thickness. In replication analyses, the congruent results were replicated to confirm our findings. Furthermore, rs3807779 SNP augmented the detrimental effect of Aβ deposition on cognitive function. Genetic profiling showed that rs3807779 has chromatin interactions with the promoter region of *MAGI2* gene, suggesting its association with *MAGI2* expression.

Conclusions: These findings demonstrate that subjects carrying the rs3807779 SNP are more susceptible to Aβ-related neurodegeneration.

Key Words: Alzheimer disease, amyloid, brain atrophy, single-nucleotide polymorphism

(*Alzheimer Dis Assoc Disord* 2020;00:000–000)

Received for publication July 21, 2020; accepted September 23, 2020.

From the *Graduate School of Medical Science & Engineering; †KAIST Institute for Health Science and Technology; ‖Department of Bio and Brain Engineering, KAIST, Daejeon; ‡Department of Neurology, Samsung Medical Center, Sungkyunkwan University School of Medicine; and §Department of Psychiatry, Asan Medical Center, University of Ulsan College of Medicine, Seoul, Republic of Korea.

Data used in the preparation of this article were obtained from the Alzheimer's Disease Neuroimaging Initiative (ADNI) database (www.adni.loni.usc.edu). As such, the investigators within the ADNI contributed to the design and implementation of ADNI and/or provided data but did not participate in analysis or writing of this report. A complete listing of ADNI investigators can be found at: http://adni.loni.usc.edu/wpcontent/uploads/how_to_apply/ ADNI_Acknowledgement_List.pdf.

Data collection and sharing for this project was funded by the ADNI (National Institutes of Health Grant U01 AG024904) and DOD ADNI (Department of Defense award number W81XWH-12-2-0012). ADNI is funded by the National Institute on Aging, the National Institute of Biomedical Imaging and Bioengineering, and through generous contributions from the following: AbbVie, Alzheimer's Association; Alzheimer's Drug Discovery Foundation; Araclon Biotech; BioClinica Inc.; Biogen; Bristol-Myers Squibb Company; CereSpir Inc.; Cogstate; Eisai Inc.; Elan Pharmaceuticals Inc.; Eli Lilly and Company; EuroImmun; F. Hoffmann-La Roche Ltd and its affiliated company Genentech Inc.; Fujirebio; GE Healthcare; IXICO Ltd; Janssen Alzheimer Immunotherapy Research & Development LLC.; Johnson & Johnson Pharmaceutical Research & Development LLC.; Lumosity; Lundbeck; Merck & Co. Inc.; Meso Scale Diagnostics LLC.; NeuroRx Research; Neurotrack Technologies; Novartis Pharmaceuticals Corporation; Pfizer Inc.; Piramal Imaging; Servier; Takeda Pharmaceutical Company; and Transition Therapeutics. The Canadian Institutes of Health Research is providing funds to support ADNI clinical sites in Canada. Private sector contributions are facilitated by the Foundation for the National Institutes of Health (www.fnih.org). The grantee organization is the Northern California Institute for Research and Education, and the study is coordinated by the Alzheimer's Therapeutic Research Institute at the University of Southern California. ADNI data are disseminated by the Laboratory for Neuro Imaging at the University of Southern California. This work was supported by Korea Health Technology Research and Development Project through the Korea Health Industry Development Institute, funded by the Ministry of Health & Welfare, Republic of Korea (HI14C2768); the Brain Research Program (2016M3C7A1913844) and Bio & Medical Technology Development Program (2016941946) through National Research Foundation of Korea, funded by the Ministry of Science and Information & Communication Technology, Republic of Korea.

The authors declare no conflicts of interest.

Reprints: Yong Jeong, MD, Laboratory for Cognitive Neuroscience and Neuroimaging, Department of Bio and Brain Engineering, Korea Advanced Institute of Science and Technology, 291 Daehak-ro, Yuseong-gu, Daejeon 34141, Republic of Korea (e-mail: yong@kaist.ac.kr).

Supplemental Digital Content is available for this article. Direct URL citations appear in the printed text and are provided in the HTML and PDF versions of this article on the journal's website, www.alzheimerjournal.com.

Amyloid β (Aβ) is a histopathologic hallmark of Alzheimer disease (AD) and its presence, measured by positron emission tomography (PET) or cerebrospinal fluid (CSF) analysis, showed a strong association with AD progression, indicating its crucial role in AD pathogenesis.[1,2] Despite the pathogenic role of Aβ in AD, a number of studies have shown a weak correlation between the level of Aβ deposition and the degree of brain atrophy,[3,4] and cognitive impairment,[5,6] suggesting individual differences in response to the accumulation of Aβ. Previous studies attributed this discrepancy to the cognitive reserve of individuals, which might compensate for damages caused by pathogenic proteins.[7] Another plausible cause is a genetic factor as previous studies have identified a number of genetic risk variants for AD.[8]

Here, we conducted a genome-wide interaction analysis to identify genetic variants that modify the effect of Aβ on brain atrophy. We expected that identification of such variants would help in understanding Aβ-related neurodegeneration and identify individuals who are susceptible or resistant to Aβ deposition.

METHODS

Subjects

Data used in the preparation of this article were obtained from the Alzheimer's Disease Neuroimaging Initiative (ADNI) database (adni.loni.usc.edu). The ADNI was

launched in 2003 as a public-private partnership, led by Principal Investigator Michael W. Weiner, MD. The primary goal of ADNI has been to test whether serial magnetic resonance imaging (MRI), PET, other biological markers, and clinical and neuropsychological assessment can be combined to measure the progression of mild cognitive impairment (MCI) and early AD. For discovery data, we included all 779 subjects (cognitively healthy controls, MCI, and AD patients) who enrolled in ADNI-GO/2, with available genetic, MRI, and Aβ ^{18}F-florbetapir PET data. For replication data, we included 129 subjects who enrolled in ADNI-1, with MRI and CSF data. The study protocol was approved by the institutional review board of each participating ADNI site (http://adni.loni.usc.edu/wp-content/uploads/how_to_apply/ADNI_Acknowledgement_List.pdf) and participants gave written informed consent for research at the time of enrollment. Baseline demographics of the 2 data sets are shown in Supplemental Table 1 (Supplemental Digital Content 1, http://links.lww.com/WAD/A308).

Image and CSF Data Acquisition

For Aβ levels measurement, we used summarized data of ^{18}F-florbetapir PET, generated from the University of California, Berkeley (version 2017.11.14). We used averaged Aβ standardized uptake value ratio value of the 4 brain regions (frontal, cingulate, lateral parietal, and lateral temporal cortex) for the global Aβ deposition value.

To measure brain atrophy, we used summarized data of cortical thickness of T1-weighted MRI, generated from the University of California, San Francisco (version 2016.8.1 for ADNI-2/GO and version 2016.2.1 for ADNI-1). Cortical reconstruction and segmentation were performed with FreeSurfer (version 4.3 in ADNI-1, version 5.1 in ADNI-2) and the cortical thickness for each of the 68 Desikan-Killiany[9] based regions of interest (ROI) were calculated (http://surfer.nmr.mgh.harvard.edu). Among 68 ROIs, we focused on the cortical thickness values of 11 AD signature regions: bilateral parahippocampus; entorhinal, fusiform, transverse, and inferior temporal cortex; postcentral, posterior cingulate, precuneus, superior, and inferior parietal cortex; and supramarginal cortex on the basis of the previous study.[10] To get the global value for cortical thickness, we used the average cortical thickness values of 11 AD signature regions. A detailed description of image preprocessing is provided in the ADNI website (http://www.adni.loni.usc/edu/data-samples/mri and http://www.adni.loni.usc/edu/data-samples/pet).

For the CSF analysis, we used the CSF data, generated in the University of Pennsylvania (version 2016.7.5) for both ADNI-GO/2 and ADNI-1. The levels of $A\beta_{1\text{-}42}$, total τ, and phosphorylated τ in the CSF were measured using a microbead-based multiplex immunoassay (INNO-BIA AlzBio3 RUO test; Fujirebio, Ghent, Belgium). Details of CSF collection are described in the ADNI website (http://www.adni.loni.usc/edu/data-samples/biospecimen-data). In the discovery data set, subset of subject (n = 667) also underwent CSF sampling. They were analyzed for the post hoc CSF data analysis. In the replication data set, a total of 129 subjects with genetic, MRI, and CSF data, who were not included in the primary analysis, were analyzed.

Finally, considering that cerebral vascular factors play an important role in AD pathogenesis,[11] we performed the post hoc analysis using white matter hyperintensities (WMH) volume data as an image marker for cerebral vascular burden. The summarized data of WMH volume (mL), generated from the University of California, Davis (version 2019.4.30) was available for the subset of the subject (n = 690) of the discovery data set. The mean time interval between WMH data and cortical thickness data were 107 days (SD, 213). WMH volume was estimated using the automated imaging procedure. Detail description of the procedure is provided in the ADNI website (http://www.adni.loni.usc/edu/data-samples/mri). We log-transformed WMH volume for the data normality.

Genotyping and Quality Control

Genetic data were collected using the Illumina HumanOmniExpress Beadchip and Illumina Human610-Quad BeadChip for ADNI-GO/2 and ADNI-1, respectively. Genotyped single-nucleotide polymorphism (SNP) were analyzed in this study. Details of collecting genome-wide association study data are provided in the ADNI website (http://www.adni.loni.usc/edu/data-samples/genetic-data). For quality control, subjects were excluded from the analysis if any of the following criteria were not satisfied: (i) call rate per subject ≥ 90% and (ii) Caucasian ethnicity (56 subjects were excluded). SNPs not meeting any of the following criteria were excluded from further analysis: (i) call rate per SNP ≥ 98% (8971 SNPs were excluded); (ii) minor allele frequency ≥ 10% (196,879 SNPs were excluded); and (iii) Hardy-Weinberg equilibrium test with *P*-value $\geq 10^{-5}$ (11,920 SNPs were excluded). After quality control, 498,606 SNPs and 723 subjects (218 cognitively healthy, 301 with MCI, and 204 with AD) remained available for the analysis. For the missing data, we conducted a sensitivity analysis with 2 extreme scenarios: all the SNPs with missing data are major allele (scenario 1) or they are minor allele (scenario 2). Primarily, we analyzed missing data using scenario 1 but also performed the same analysis using scenario 2. The result of scenario 2 is described in the Supplemental Material (Supplemental Digital Content 2, http://links.lww.com/WAD/A309).

Statistical Analysis

Genome-wide Interaction Analysis

In a genome-wide interaction analysis, we used a linear regression model with the global cortical thickness value as the quantitative outcome measure. We included Aβ, SNP (0, 1, and 2 as the number of minor allele), and Aβ × SNP interactions as predictors, and age, sex, level of education, diagnosis (as dummy variable indicating healthy cognition, MCI, or AD), *APOE* genotype (0, 1, and 2 as the number of ε4 allele), and intracranial volume as covariates. Lastly, in order to control for the subpopulation effect, we performed principal component (PC) analysis using the subjects' SNP data and included the first 4 PCs in the regression model as a covariate. This method is widely used to correct the population structure.[12] Our term of interest was the Aβ × SNP interaction, which was used to identify SNPs that modify the relationship between global cortical thickness and global Aβ deposition. In the genome-wide interaction analysis, we defined a *P*-value (2-tailed) $<5\times10^{-8}$ as being statistically significant (genome-wide significant) and 1×10^{-6} as being statistically suggestive (genome-wide suggestive), which are based on performing a Bonferroni correction of all the independent common SNPs across the human genome.[13] We assessed and controlled the genomic inflation on the basis of the previous study.[14] In the replication analysis, we used the level of CSF $A\beta_{1\text{-}42}$ as the global Aβ value in the

linear regression model and performed the analysis for identified SNPs from primary analysis. For the replication results, 1-tailed *P*-values are reported given the expectation for effects in the same direction with result from the discovery data set.

Post Hoc Analysis

After identifying the significant SNP and Aβ interactions, we performed the region-wide interaction analysis. In this analysis, we used cortical thickness values of all 68 ROIs as outcome measures and calculated the regional β coefficient of Aβ × SNP interactions after adjusting the effects of age, sex, level of education, diagnosis, *APOE* ε4 genotype, intracranial volume, and genetic PCs. From this analysis, we could spatially localize the Aβ and SNP interaction effect in the brain. *P*-value <0.0007 is defined as statistically significant on the basis of a Bonferroni correction (0.05/68 = 0.0007).

We stratified subjects by the presence of the SNP and compared their baseline demographics and the degree of AD pathology. Comparative and interaction analysis were also performed at the subgroup level by the baseline diagnosis. In addition, we assessed whether the SNP also altered the effect of Aβ on cognitive function. We used the mini-mental state examination score as the quantitative cognitive measure in the linear regression analysis (adjusted for age, sex, level of education, diagnosis, and *APOE* genotype). Furthermore, we assessed whether the SNP also altered the effect of τ on brain atrophy using CSF data. For the post hoc analysis of WMH, we first performed the linear regression analysis to evaluate whether WMN volume is associated with global cortical thickness value. Then, we added WMH volume as a covariate in the subsequent analysis to evaluate whether the interaction effect of SNP is significant after adjusting the effect of WMH. Post hoc analysis, excluding the region-wide interaction analysis, defined *P*-value <0.05 as statistically significant.

Functional Characterization of the Identified SNP

Finally, in order to characterize the function of identified SNP, we leveraged bioinformatics tools such as linkage disequilibrium (LD), high-throughput chromosome conformation capture (Hi-C), and gene expression pattern analysis. We used LDlink,[15] an online tool on the basis of Phase 3 of the 1000 Genomes Project, and dbSNP build 142, to explore SNPs that were in LD ($R^2 > 0.7$) with the SNP of interest. We utilized the Hi-C data from hippocampal tissue[16] to detect genomic regions that exhibited long-range chromatin interactions with the SNP of interest. Bias-normalized and distance-normalized interaction frequencies were assessed for the bin (5 kb in size) harboring the SNP of interest. We used bedtools (version 2.27.0) for the intersection of the SNPs and Bioconductor package Gviz in R for data visualization.[17–19] Lastly, we examined gene expression in multiple tissues using the Genotype-Tissue Expression project data.[20]

Availability of Data and Materials

We used R software (http://www.r-project.org) and MATLAB (Mathworks 2014b, http://www.mathworks.com) for the statistical analyses and result visualization. The data set supporting the conclusions of genome-wide interaction analysis is available in the ADNI public database (http://adni.loni.usc.edu/data-samples/access-data/). Anonymized patient identification numbers, imaging, genetic, and biospecimen data are available from the ADNI database at the request of qualified researchers. The data set supporting the conclusion of post hoc analysis is available in databases of Gene Expression Omnibus (https://www.ncbi.nlm.nih.gov/geo/) and Genotype-Tissue Expression Project (https://www.gtexportal.org/home/).

RESULTS

Genome-wide Interaction Analysis

Before the interaction analysis, we demonstrated that there was a significant association between global Aβ level with global cortical thickness value (β = −0.08, SE = 0.02, *P* = 0.0014 for Aβ PET; β = 0.0008, SE = 0.0002, *P* = 0.00018 for CSF $A\beta_{1\text{-}42}$) in the linear regression model after adjusting the effects of age, sex, level of education, diagnosis, *APOE* ε4 genotype, and intracranial volume.

Genome-wide interaction analysis identified, 2 SNPs (rs10922610 and rs3807779) of genome-wide suggestive interactions with Aβ (rs10926610, $P = 1.86\times10^{-7}$; rs3807779, $P = 9.08\times10^{-7}$; Fig. 1A). A quantile-quantile plot of *P*-values revealed some genomic inflation (λ = 1.1; Fig. 1B). After controlling the genomic inflation, *P*-values were 4.27×10^{-7} and 1.74×10^{-6} for rs10922610 and rs3807779, respectively. In the replication analysis, only rs3807779 showed significant interaction with CSF $A\beta_{1\text{-}42}$ on brain atrophy (*P* = 0.038).

Post Hoc Analysis

Because the rs3807779 SNP were consistently identified in 2 independent data set (ADNI-GO/2 and ADNI-1), we focused the post hoc analysis on this SNP. In the model, the rs3807779 × Aβ interaction term showed a negative β coefficient (β = −0.14, SE = 0.02, *t* = −4.95), indicating that the subjects with a higher number of minor allele show a stronger negative correlation between Aβ level and global cortical thickness value (Fig. 2A). The region-wide interaction analysis identified significant Aβ and rs3807779 interactions on 17 cortical regions in temporoparietal area (Fig. 3; Supplemental Table 2, Supplemental Digital Content 3, http://links.lww.com/WAD/A310).

Subjects with and without the rs3807779 SNP did not show any significant differences in baseline demographics and the level of AD pathologies (Table 1). However, in the subgroup analysis, AD patients with the rs3807779 SNP showed lower global cortical thickness than those without the SNP (Supplemental Table 3, Supplemental Digital Content 4, http://links.lww.com/WAD/A311). Furthermore, there were significant rs3807779 and Aβ interaction in all 3 diagnostic groups (Supplemental Table 4, Supplemental Digital Content 4, http://links.lww.com/WAD/A311). In regard to cognitive function, cortical Aβ was related to poor cognitive performance, and this relationship was augmented in subjects with the rs3807779 SNP (*P* = 0.00082) (Fig. 2B). In the CSF analysis, the levels of $A\beta_{1\text{-}42}$ and total τ in the CSF also showed a significant interaction with rs3807779 on brain atrophy ($A\beta_{1\text{-}42}$, *P* = 0.0005; total τ, *P* = 0.0002; Supplemental Fig. 1, Supplemental Digital Content 5, http://links.lww.com/WAD/A312), whereas the levels of phosphorylated τ showed insignificant interaction (*P* = 0.09). There was no significant rs3807779 and Aβ interaction (from either PET or CSF) on the levels of CSF total or phosphorylated τ.

In the post hoc study of WMH, there were a significant association between WMH volume with global cortical thickness value (β = −0.018, SE = 0.004, *P* = 0.0002) after

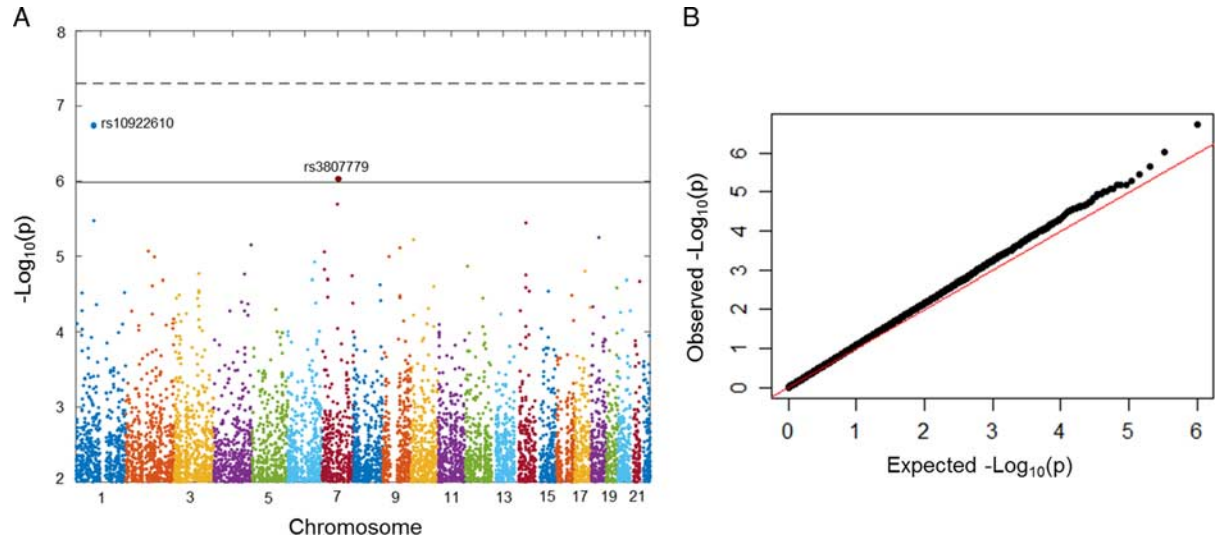

FIGURE 1. Results of genome-wide interaction analysis. A, Manhattan plot showing single-nucleotide polymorphism and amyloid β interactions at rs10922610 and rs3807779 are associated with brain atrophy. B, Quantile-quantile plot showing the presence of genomic inflation. Dotted line indicates the genome-wide significance level ($P = 5\times10^{-8}$). Solid line indicates the genome-wide suggestive level ($P = 1\times10^{-6}$).

controlling the effects of age, sex, level of education, diagnosis, *APOE* ε4 genotype, and intracranial volume. When we included WMH volume as a covariate in the interaction analysis, Aβ and rs3807779 interaction remained significant (β = −0.14, SE = 0.02, $P = 2.97\times10^{-6}$).

Functional Characterization of rs3807779

rs3807779 (major allele = cytosine; minor allele = thymine) was mapped to an intron of the *MAGI2* gene. Located at chromosome 7q21.11, this gene encodes for membrane-associated guanylate kinase inverted 2 (MAGI2). We identified SNPs in LD with rs3807779 (Fig. 4A) and verified the potential target regions of the identified SNPs through Hi-C data generated in hippocampal tissue. The bin including rs3807779 showed strong (distance-normalized interaction frequency > 4) interaction with bins located near the promoter region of *MAGI2* (Fig. 4B), suggesting a functional role of the identified SNPs. When we examined gene expression patterns, *MAGI2* showed a high level of gene expression in the cerebral cortex and hippocampus with 15 and 12 transcripts per million expression values respectively, while showed a low level of gene expression in other tissues (Fig. 4C).

DISCUSSION

We identified a SNP at rs3807779 that modifies the effect of Aβ deposition on brain atrophy. We found that a greater dosage of the rs3807779 minor allele causes a stronger association between global Aβ deposition and global cortical thickness.

The region-wide interaction study revealed significant Aβ and rs3807779 interaction on 17 cortical regions in

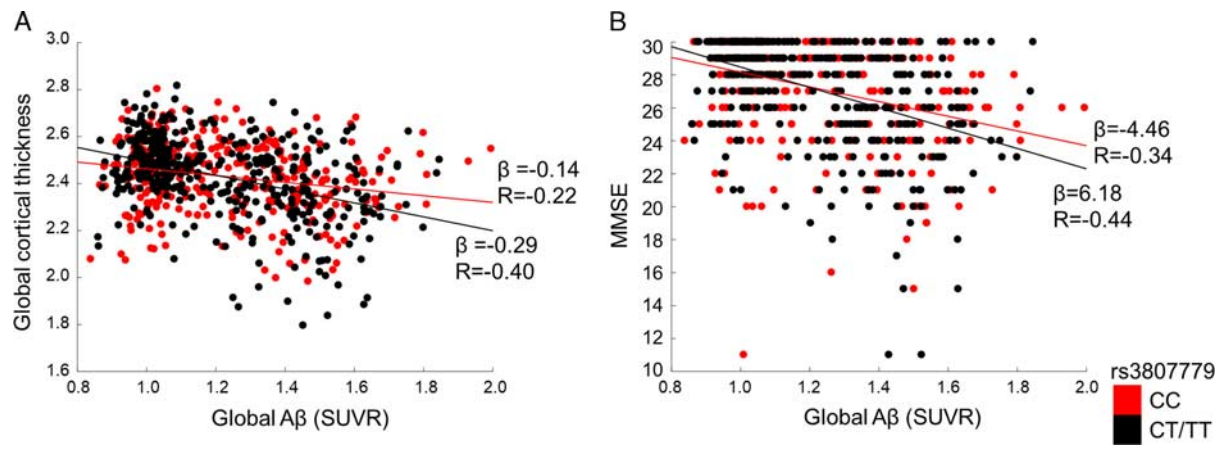

FIGURE 2. Scatter plots of Alzheimer disease biomarkers in subjects stratified by rs3807779 single-nucleotide polymorphism (SNP). A, Scatter plot and best-fit line showing correlations between global amyloid β (Aβ) deposition on positron emission tomography (PET) and the global cortical thickness on magnetic resonance imaging in subjects stratified by the rs3807779 SNP. B, Scatter plot and best-fit line showing the correlations between the global Aβ deposition on the PET and mini-mental state examination (MMSE) score in subjects stratified by the rs3807779 SNP. The *R* and β coefficients were calculated using linear regression analysis. SUVR indicates standardized uptake value ratio.

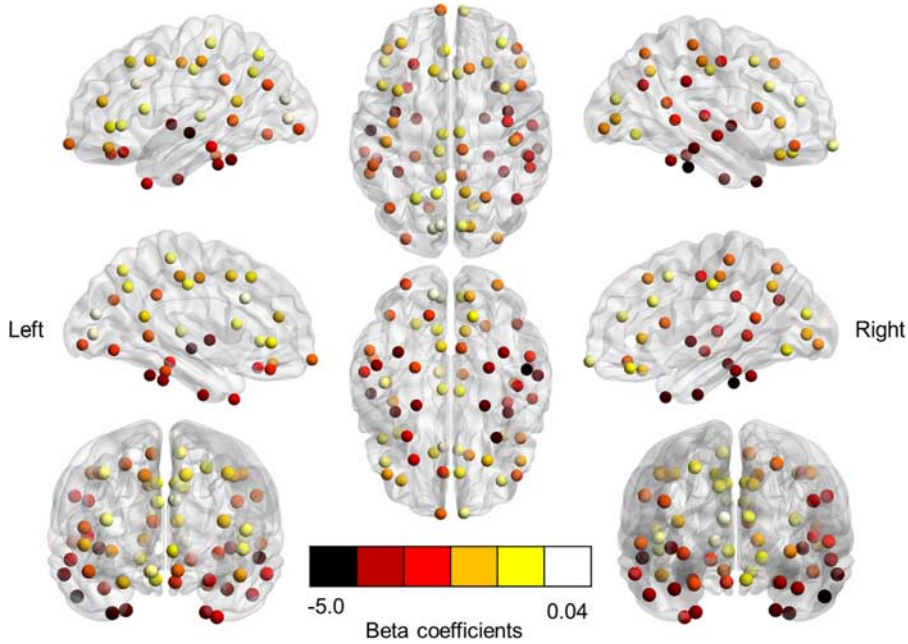

FIGURE 3. Region-wide interaction analysis. β coefficient map showing high amyloid β and rs3807779 interaction on the cortical thickness of bilateral temporal and posterior parietal regions.

temporoparietal area, which correspond to the typical AD atrophy pattern.[21] Although there were significant rs3807779 and Aβ interactions in all diagnostic groups, the decreased cortical thickness in subjects carrying rs3807779 SNP was present only in AD. Given that the detrimental effects of rs3807779 on cortical thickness are mediated through Aβ deposition, we speculated that the decreased cortical thickness only in the advanced disease state could be attributed to the level of Aβ accumulation in the brain.

An interaction was also found for cognitive function but with a smaller effect size than for brain structure. This is in line with biomarker modeling in AD, which indicates that brain atrophy occurs closer in time to the deposition of Aβ.[22] Thus, the phenotypic effects of genetic variants on Aβ would first become evident in brain structure before any cognitive decline can be observed. Furthermore, cognitive decline in elderly subjects is not only caused by AD but also by a variety of factors, including medication, mood states, education level, and literacy.[23] Thus, the genetic effect on cognitive function could be obscured by these factors.

Interestingly, there was a significant interaction effect of rs3807779 and CSF τ levels on brain atrophy. We also evaluated the rs3807779 and Aβ interaction on changes of CSF τ level in order to assess whether the increased detrimental effect of Aβ on cortical thickness in subject carrying rs3807779 was through an increase in τ level. As a result, there was no significant interaction. These findings suggesting that the rs3807779 and Aβ interaction is not mediated by changes in τ levels, but that the rs3807779 SNP augments the detrimental effect of Aβ and of τ on the cortical thickness.

In this study, 35% of the participants carried 1 or more rs3807779 minor alleles. This is in accordance with previous studies, indicating that the samples used in this study, are not biased and may be representative of the whole Caucasian population.[24] Although the molecular mechanism by which rs3807779 SNP affects the pathogenesis of AD is not evaluated, some possible explanations can be inferred from the genetic profile of this SNP. We found that rs3807779 and LD-linked SNPs were all mapped on *MAGI2*. Furthermore, by leveraging the 3-dimensional chromatin structure, we found that these SNPs had chromatin interactions with the promoter region of *MAGI2* in the hippocampal tissue.

TABLE 1. Comparison Between Subjects by rs3807779 SNP

rs3807779	CC (n = 335)	CT or TT (n = 388)	*P*
Age, mean (SD) (y)	73.91 (7.1)	74.04 (7.3)	0.808
Female, n (%)	142 (42.6)	190 (49)	0.085
Education, mean (SD) (y)	16.3 (2.62)	16.16 (2.6)	0.492
MMSE, score (SD)	27.15 (3.06)	27.13 (3.23)	0.940
Presence of ε4 allele of *APOE*, n (%)*	146 (43.8)	176 (45.8)	0.599
Diagnosis (HC/MCI/AD)	101/135/99	117/166/105	0.734
Global cortical thickness, mean (SD)	2.43 (0.15)	2.43 (0.16)	0.998
Global Aβ, SUVR, mean (SD)	1.22 (0.23)	1.21 (0.23)	0.550
CSF $A\beta_{1-42}$, mean (SD) (pq/mL)†	236.58 (88.06)	249.41 (92.33)	0.107
CSF total τ, mean (SD) (pq/mL)†	78.24 (44.30)	81.58 (48.11)	0.361
CSF p-τ, mean (SD) (pq/mL)†	25.61 (13.49)	26.10 (13.56)	0.581
Time interval, mean (SD) (d)‡	17.99 (28.72)	18.16 (50.74)	0.956

*Subjects has 1 or more ε4 allele

†In total, 667 subjects were included in analysis of CSF data.

‡Time interval between Aβ positron emission tomography and the magnetic resonance imaging.

Aβ indicates amyloid β; AD, Alzheimer disease; CSF, cerebrospinal fluid; HC, healthy control; MCI, mild cognitive impairment; MMSE, mini-mental state examination; p-τ, phosphorylated τ; SNP, single-nucleotide polymorphism; SUVR, standardized uptake value ratio.

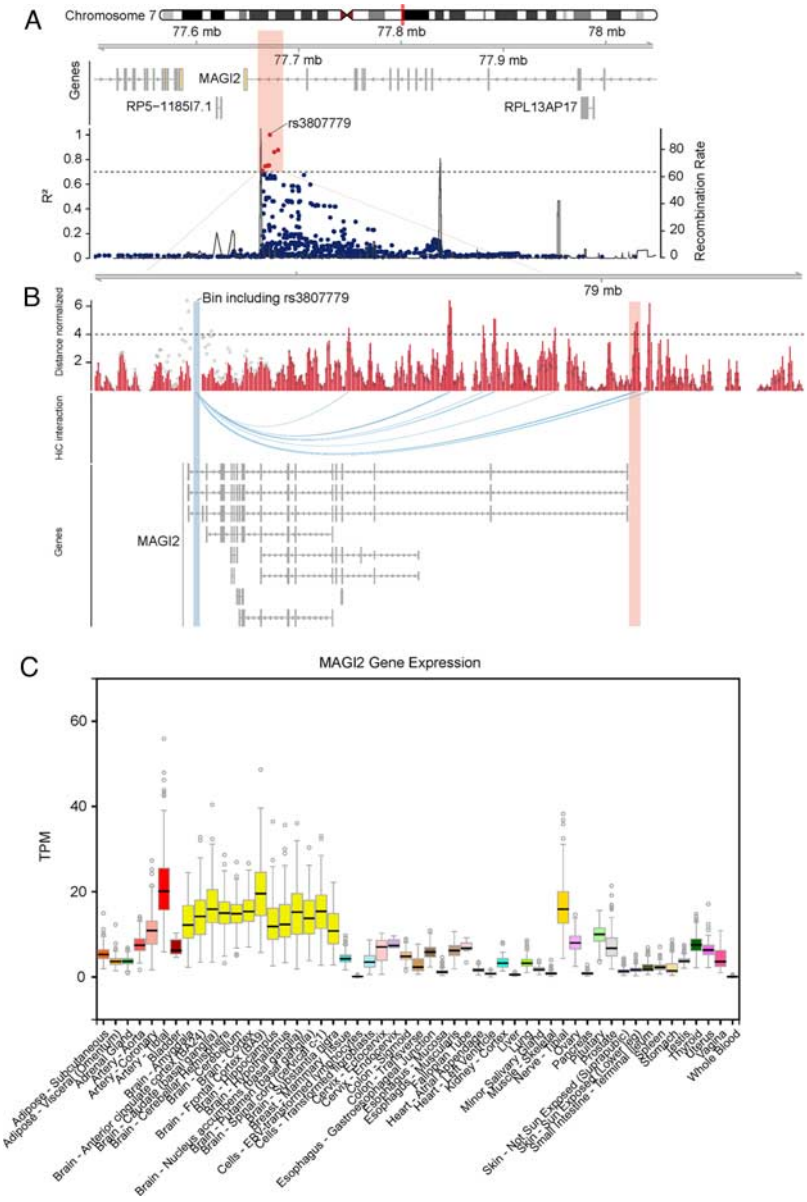

FIGURE 4. Functional characterization of rs3807779. A, Chromosomal map showing the location of the rs3807779 single-nucleotide polymorphism at a recombination hotspot in an intron of *MAGI2*. B, High-throughput chromosome conformation capture (Hi-C) data in hippocampal brain revealing chromatin interactions between the rs3807779 locus and the promoter region of MAGI2. The blue curves represent Hi-C interactions between the 5 Kb bins for the rs3807779 locus and the promoter at distance-normalized interaction frequency > 4. C, Expression of MAGI2 in various tissues. MAGI2 is highly expressed in brain tissues. The figure was generated from the Genotype-Tissue Expression portal (https://www.gtexportal.org/home).

Although the specific biological mechanism studies are further required, these findings suggest that *MAGI2* gene may be a possible link between rs3807779 SNP and the Aβ-related neurodegeneration.

MAGI2 is a cell membrane-associated protein, characterized by 2 WW domains, a guanylate kinase-like domain, and multiple PDZ domains. It is highly expressed in the brain and maintains neuronal structure and function by acting as a scaffolding protein at neuronal synapses by assembling neurotransmitter receptors and cell adhesion proteins.[25,26] *MAGI2* variants have been reported in several brain disorders, including dentato-rubral and pallidoluysian atrophy,[27] infantile spasm,[28] schizophrenia,[29] and AD.[30] One prior study showed that the common genetic variant of *MAGI2* is associated with hippocampal atrophy in AD.[31] In our study, we demonstrated comparable results; the global cortical thickness was lower in AD patients carrying the rs3807779 SNP than in those without the SNP. Thus the enhanced brain atrophy found in the prior study[31] may be due to the greater negative effect of Aβ deposition on brain structure in subjects carrying the genetic variant of *MAGI2*.

MAGI2 is also considered to assemble ubiquitination enzymes to plasma membrane proteins. The ubiquitin system is responsible for the degradation of misfolded or abnormal proteins,[32] and its impairment has been reported in AD.[33] Therefore, the genetic variant of *MAGI2* might

exaggerate the neurodegeneration in AD by perturbing neuronal integrity and the ubiquitin system.

This study has some limitations. First, the sample size was small. Thus, the statistical significance of our results was small at the genome-wide suggestive level. Moreover, we observed some genomic inflation in our data, which might lead to an overestimation of the statistical significance level. Therefore, our findings should be cautiously interpreted given the potential for false positives. However, a previous study showed that common SNPs (minor allele frequency $> 10\%$) exhibit significantly fewer false-positive results than expected by chance at less stringent *P*-value thresholds.[34] Furthermore, the nominal replication by an independent data set and the biological relevance of the identified SNPs in functional analyses suggest that our study less likely presented false-positive results. Second, we could not evaluate the causality of the observed results with the current analysis. By using available data on the identified SNP and *MAGI2*, we can only speculate that rs3807779 interferes with the expression of *MAGI2* and enhances neurodegeneration in AD by impairing neuronal integrity and intracellular clearing systems. Further studies are required to solve these issues. Lastly, τ level was only measured in CSF in this study. As τ PET (^{18}F-AV1451) is available only for a subset of participants in the ADNI data set, it can be used in the future studies.

CONCLUSIONS

We identified a common genetic variant in *MAGI2* that modifies the effect of Aβ deposition on brain atrophy. Our findings demonstrated that subjects carrying the rs3807779 SNP are more susceptible to Aβ-related neurodegeneration.

REFERENCES

1. Hansson O, Zetterberg H, Buchhave P, et al. Association between CSF biomarkers and incipient Alzheimer's disease in patients with mild cognitive impairment: a follow-up study. *Lancet Neurol*. 2006;5:228–234.
2. Morris JC, Roe CM, Grant EA, et al. Pittsburgh compound B imaging and prediction of progression from cognitive normality to symptomatic Alzheimer disease. *Arch Neurol*. 2009; 66:1469–1475.
3. Bennett DA, Schneider JA, Wilson RS, et al. Neurofibrillary tangles mediate the association of amyloid load with clinical Alzheimer disease and level of cognitive function. *Arch Neurol*. 2004;61:378–384.
4. Giannakopoulos P, Herrmann F, Bussiere T, et al. Tangle and neuron numbers, but not amyloid load, predict cognitive status in Alzheimer's disease. *Neurology*. 2003;60:1495–1500.
5. Bennett D, Schneider J, Arvanitakis Z, et al. Neuropathology of older persons without cognitive impairment from two community-based studies. *Neurology*. 2006;66:1837–1844.
6. Nelson PT, Braak H, Markesbery WR. Neuropathology and cognitive impairment in Alzheimer disease: a complex but coherent relationship. *J Neuropathol Exp Neurol*. 2009;68:1–14.
7. Stern Y. Cognitive reserve in ageing and Alzheimer's disease. *Lancet Neurol*. 2012;11:1006–1012.
8. Bettens K, Sleegers K, Van Broeckhoven C. Genetic insights in Alzheimer's disease. *Lancet Neurol*. 2013;12:92–104.
9. Desikan RS, Ségonne F, Fischl B, et al. An automated labeling system for subdividing the human cerebral cortex on MRI scans into gyral based regions of interest. *Neuroimage*. 2006;31:968–980.
10. Wang L, Benzinger TL, Hassenstab J, et al. Spatially distinct atrophy is linked to β-amyloid and tau in preclinical Alzheimer disease. *Neurology*. 2015;84:1254–1260.
11. Marchant NL, Read RB, DeCarli CS, et al. Cerebrovascular disease, beta-amyloid, and cognition in aging. *Neurobiol Aging*. 2012;33:1006–e25.
12. Price AL, Patterson NJ, Plenge RM, et al. Principal components analysis corrects for stratification in genome-wide association studies. *Nat Genet*. 2006;38:904–909.
13. Xu CJ, Tachnazidou I, Walter K, et al. Estimating genome-wide significance for whole-genome sequencing studies. *Genet Epidemiol*. 2014;38:281–290.
14. van Iterson M, van Zwet EW, Heijmans BT. Controlling bias and inflation in epigenome-and transcriptome-wide association studies using the empirical null distribution. *Genome Biol*. 2017;18:19.
15. Machiela MJ, Chanock SJ. LDlink: a web-based application for exploring population-specific haplotype structure and linking correlated alleles of possible functional variants. *Bioinformatics*. 2015;31:3555–3557.
16. Yang D, Jang I, Choi J, et al. 3DIV: a 3D-genome Interaction Viewer and database. *Nucleic Acids Res*. 2017;46:D52–D57.
17. Lieberman-Aiden E, Van Berkum NL, Williams L, et al. Comprehensive mapping of long-range interactions reveals folding principles of the human genome. *Science*. 2009;326:289–293.
18. Marchini J, Howie B, Myers S, et al. A new multipoint method for genome-wide association studies by imputation of genotypes. *Nat Genet*. 2007;39:906–913.
19. Neph S, Vierstra J, Stergachis AB, et al. An expansive human regulatory lexicon encoded in transcription factor footprints. *Nature*. 2012;489:83–90.
20. Lonsdale J, Thomas J, Salvatore M, et al. The genotype-tissue expression (GTEx) project. *Nat Genet*. 2013;45:580–585.
21. Veitch DP, Weiner MW, Aisen PS, et al. Understanding disease progression and improving Alzheimer's disease clinical trials: recent highlights from the Alzheimer's Disease Neuroimaging Initiative. *Alzheimers Dement*. 2019;15:106–152.
22. Jack CR, Knopman DS, Jagust WJ, et al. Tracking pathophysiological processes in Alzheimer's disease: an updated hypothetical model of dynamic biomarkers. *Lancet Neurol*. 2013;12: 207–216.
23. Fillenbaum G, Hughes D, Heyman A, et al. Relationship of health and demographic characteristics to mini-mental state examination score among community residents. *Psychol Med*. 1988;18:719–726.
24. Sherry ST, Ward M-H, Kholodov M, et al. dbSNP: the NCBI database of genetic variation. *Nucleic Acids Res*. 2001;29:308–311.
25. Deng F, Price MG, Davis CF, et al. Stargazin and other transmembrane AMPA receptor regulating proteins interact with synaptic scaffolding protein MAGI-2 in brain. *J Neurosci*. 2006;26:7875–7884.
26. Hirao K, Hata Y, Yao I, et al. Three isoforms of synaptic scaffolding molecule and their characterization multimerization between the isoforms and their interaction with N-methyl-D-aspartate receptor and SAP90/PSD-95-associated protein. *J Biol Chem*. 2000;275:2966–2972.
27. Wood JD, Yuan J, Margolis RL, et al. Atrophin-1, the DRPLA gene product, interacts with two families of WW domain-containing proteins. *Mol Cell Neurosci*. 1998;11:149–160.
28. Marshall CR, Young EJ, Pani AM, et al. Infantile spasms is associated with deletion of the MAGI2 gene on chromosome 7q11. 23-q21. 11. *Am J Hum Genet*. 2008;83:106–111.
29. Koide T, Banno M, Aleksic B, et al. Common variants in MAGI2 gene are associated with increased risk for cognitive impairment in schizophrenic patients. *PloS One*. 2012;7:e36836.
30. Sekine M, Makino T. Inference of causative genes for Alzheimer's disease due to dosage imbalance. *Mol Biol Evol*. 2017;34:2396–2407.
31. Potkin SG, Guffanti G, Lakatos A, et al. Hippocampal atrophy as a quantitative trait in a genome-wide association study identifying novel susceptibility genes for Alzheimer's disease. *PloS One*. 2009;4:e6501.
32. Bence NF, Sampat RM, Kopito RR. Impairment of the ubiquitin-proteasome system by protein aggregation. *Science*. 2001;292:1552–1555.
33. Hong L, Huang H-C, Jiang Z-F. Relationship between amyloid-beta and the ubiquitin–proteasome system in Alzheimer's disease. *Neurol Res*. 2014;36:276–282.
34. Tabangin ME, Woo JG, Martin LJ. The effect of minor allele frequency on the likelihood of obtaining false positives. *BMC Proc*. 2009;3(suppl 7):S41.